

# DITEC

## *Experimental Analysis of an Image Characterization Method based on the Trace Transform*

Igor G. Olaizola<sup>1</sup>, Iñigo Barandiaran<sup>1</sup>, Basilio Sierra<sup>2</sup> and Manuel Graña<sup>2</sup>

<sup>1</sup>*Vicomtech-IK4 Research Alliance, Donostia, Spain*

<sup>2</sup>*Dpto. CCIA, UPV-EHU, Donostia, Spain*

**Keywords:** Feature Descriptor, Trace Transform, Image Matching, Image Characterization.

**Abstract:** Global and local image feature extraction is one of the most common tasks in computer vision since they provide the basic information for further processes, and can be employed on several applications such as image search & retrieval, object recognition, 3D reconstruction, augmented reality, etc. The main parameters to evaluate a feature extraction algorithm are its discriminant capability, robustness and invariance behavior to certain transformations. However, other aspects such as computational performance or provided feature length can be crucial for domain specific applications with specific constraints (real-time, massive datasets, etc.). In this paper, we analyze the main characteristics of the DITEC method used both as global and local descriptor method. Our results show that DITEC can be effectively applied in both contexts.

## 1 INTRODUCTION

Image analysis and characterization tasks used for applications like image search & retrieval, 3D reconstruction, or augmented reality are mainly based on the extraction of *low-level features* as primary information units for its further processes. These features can be obtained either by analyzing specific characteristics of the whole image (global features) or by processing points or areas with relevant information (local features). While image characterization can be performed by using both types of features, some other tasks such as stereo disparity estimation, image stitching, or camera tracking require the detection, description and matching of interesting points. Key point extraction and description mechanisms play a key role during image matching process, where several image points must be accurately identified to robustly estimate a transformation or recognize an object.

In this paper we analyze the behavior as both a global and a local descriptor of a novel method (DITEC) which has been already successfully tested as global approach in image characterization tasks (Olaizola et al., 2012). The very promising results obtained in the evaluation phase suggest its potential as a highly discriminative local descriptor.

The paper is structured as follows: section 2 gives a brief description on previous work related with im-

age description or characterization. Section 3 describes our DITEC approach and the methodology used for the evaluation of DITEC, performing as both global and local descriptor. Section 4 describes results obtained by DITEC approach compared with similar approaches, both globally (Section 4.1) and locally (Section 4.2). Finally, Section 5 gives final remarks and future work.

## 2 RELATED WORK

### 2.1 Image Descriptors

There is a vast literature regarding different global features. Histograms of several local features (Bouker and Hervet, 2011), texture features (Manjunath et al., 1998) or self similarity (Shechtman and Irani, 2007) have been broadly used as low level features for image characterization. Watanabe et al. (Watanabe et al., 2002) proposed a global descriptor based on the code-words provided by Lempel-Ziv (Ahmed et al., 2011; Cerra et al., 2010) entropy coders assuming that the codification of the complexity of data can characterize the content represented within it. Among all these global descriptors, DITEC has proven to be a very promising method for robust image domain categor-

rization, producing short codewords with a high discriminant value.

In addition to globally describing images, local approaches are also becoming an active topic in research community. Local descriptors are nowadays widely used by computer vision community (Snoek and Smeulders, 2010). Some approaches such as SIFT (Lowe, 1999) are extensively used in many computer vision based applications because of their robustness. However, the application of such approaches in contexts like real-time image processing, are not suitable due to its computation requirements. Some other approaches such as SURF (Bay et al., 2006a) or BRIEF (Calonder et al., 2010a) overcome this computational requirements, being some of the most popular approaches when near real-time performance is required. Usually, a trade-off between robustness and performance needs to be tackled.

### 2.2 Trace Transform

The trace transform has been already used for several computer vision applications. MPEG-7 (Martínez, 2004) standard specification for image fingerprinting contains a method based on the trace transform to create hash codes (Bober and Oami, 2007; O’Callaghan et al., 2008). Other applications such as face recognition (Fahmy, 2006; Srisuk et al., 2003; Liu and Wang, 2007; Liu and Wang, 2009), character recognition (Nasrudin et al., 2010) and sign recognition (Turan et al., 2005) are other examples where the trace transform was successfully applied.

The data transformation process is carried out through the trace transform, a generalization of the Radon transform (1) where the integral of the function is substituted for any other functional  $\Xi$  (Kadyrov and Petrou, 1998; Kadyrov and Petrou, 2001; Petrou and Kadyrov, 2004; Turan et al., 2005; Brasnett and Bober, 2008).

$$R(\phi, \rho) = \iint f(x, y) \delta(x \cos \phi + y \sin \phi - \rho) dx dy \quad (1)$$

The trace transform consists in applying a functional  $\Xi$  along a straight line (L in Figure 1). This line is moved tangentially to a circle of radius  $\rho$  covering the set of all tangential lines defined by  $\phi$ . The Radon transform has been used to characterize images (Peyrin and Goutte, 1992) in well defined domains (Lin et al., 2010), in image fingerprinting (Seo et al., 2004) and as a primitive feature for general image description. The trace transform extends the Radon transform by enabling the definition of the functional and thus enhancing the control on the feature space. These features can be set up to show scale, rotation,

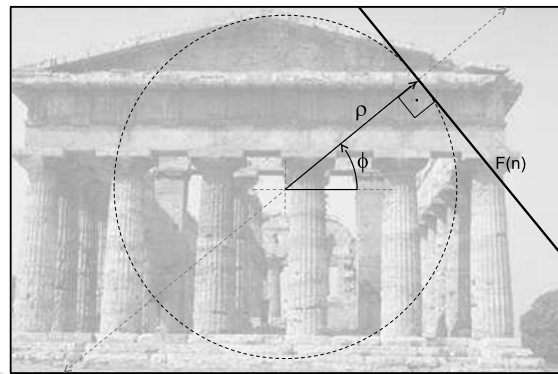


Figure 1: Trace transform, geometrical representation (Olaizola et al., 2012).

affine transformation invariance or high discriminative capacity for specific content domains.

### 3 METHODS

DITEC method proposed in (Olaizola et al., 2012) consists of a method based on the trace transform to extract efficient global descriptors for domain categorization. The results of DITEC tested with Corel 1000 dataset<sup>1</sup> and a subset of Geoeye<sup>2</sup> show its potential as global feature for image characterization.

In addition to global image descriptors, an image can also be categorized or described by extracting local information in several positions along its dimensions. This local information is usually represented in form of local descriptors. A local image descriptor can be seen as a vector of values representing a region of size  $s$  around a detected key point  $p$ , as shown in figure 2. The type of data and vector dimensions depends on the nature of the local description algorithm.

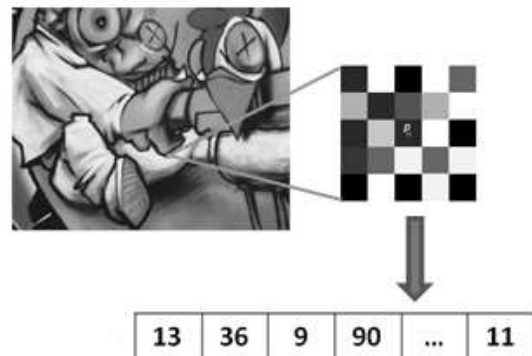


Figure 2: Local image patch and corresponding local descriptor.

<sup>1</sup>Corel Gallery Magic 65000 (1999), www.corel.com

<sup>2</sup>http://www.geoeeye.com

For example, one of the most successful descriptor to date, SIFT (Lowe, 1999), is represented as a vector of 128 floating point values. Our local image descriptor approach works on single channel images, thus no color information is used. Many of the most popular local image descriptors, such as SIFT (Lowe, 1999), SURF (Bay et al., 2006b) or BRIEF (Calonder et al., 2010b) use also intensity information only. As mentioned before, DITEC algorithm is an approach for image description, thus an additional mechanism for interest point detection or segmentation is needed, in order to apply it locally. In order for DITEC to obtain high robustness to scale transformation, a detector with key point scale  $s$  estimation is needed. In the current evaluation, we used as interest point extraction, the detection of local maxima in scale-space of Laplacian of Gaussian (LoG), approximated by difference of Gaussians (Lowe, 1999).

Once key points are detected, we apply DITEC approach locally to every detected points. In this way,  $n$  image patches of size  $s$ , proportional to the scale estimated by the point detector, are extracted around each key point  $x_i$ . These patches are reduced bi-linearly to a predefined size  $n$ . Then, for every patch, a trace transform  $g(\phi, \rho)$  with a given functional  $F$  is computed.  $g(\phi, \rho)$  is then normalized between 0 and 1 in order to reduce the influence of signal intensity and make DITEC robust against light intensity variations. Once the trace transform is normalized, the frequential coefficients of the patch are obtained.

## 4 EVALUATION

### 4.1 Behavior as Global Descriptor

The analysis of DITEC as global feature extraction method for image domain characterization has been performed using three different datasets. The experiments with the first two datasets (Geoeye and Corel 1000) are described in (Olaizola et al., 2012) while a more detailed analysis of the results is presented here. The third experiment has been performed on a new dataset composed by a subset of Caltec 101 (described in Section 4.1.3). These three datasets allow the evaluation of the method under different conditions in terms of type of content domains, variations in resolution, etc.

#### 4.1.1 Corel 1000

Corel 1000 dataset is composed of 10 different classes with 1000 instances per class where some classes represent scenes while some other represent specific ob-

jects within a scene and few of them are more related to specific objects contained within a scene. The best precision results for this datasets are shown in Table 1. The general precision achieved for Corel 1000 is 84.8%. A non square resolution of  $n_\phi$  and  $n_\rho$  has been used in this case. The low angular resolution reduces the rotational invariance of the descriptor, a constraint that is not required for this dataset. In this case the average value has been applied as functional and the SVM implementation of Weka 3.6.4 (SMO) has been used for training and classification.

Table 1: Corel 1000 dataset confusion matrix. The closest classes attending the misclassification rates are represented in bold.

	a	b	c	d	e	f	g	h	i	j
a) Africans	75	2	6	0	2	5	0	2	1	7
b) Beach	5	79	6	1	0	6	0	0	<b>2</b>	1
c) Architecture	3	4	78	1	0	3	1	0	8	2
d) Buses	3	3	3	81	0	0	1	0	4	5
e) Dinosaurs	0	0	0	0	100	0	0	0	0	0
f) Elephants	7	1	3	0	0	83	0	2	3	1
g) Flowers	1	1	0	0	0	0	95	2	0	1
h) Horses	1	0	1	1	0	0	0	97	0	0
i) Mountains	0	<b>14</b>	4	1	0	3	0	0	78	0
j) Food	5	1	0	5	0	3	4	0	0	82

A deeper analysis of Corel 1000 has been performed by analyzing the 224 attributes obtained during an evolutionary feature selection process. These remaining 224 attributes have been analyzed and ranked with a Support Vector Machine (SVM) classifier. The ranking criteria has been the square of the weight assigned by the SVM classifier (Guyon et al., 2002). Then an iterative test has been performed starting from the five most important values and increasing the number of attributes according to the rank obtained previously. The obtained results can be observed in Figure 3. This evaluation shows that there are few attributes with strong discriminative power. When the number of attributes reaches around 180, the precision starts decreasing.

SVM based attribute selection has some drawbacks in terms of computational performance and data sensitivity. A more robust approach for feature extraction can be provided by Principal Component Analysis (PCA), also known as Karhunen-Loève transform (Bishop, 2006). The goal of this approach is to project data onto a space with a lower dimensionality, while maximizing the variance of the projected data.

As it can be seen in Figure 3, PCA method improves the precision for dimensionalities below 14,

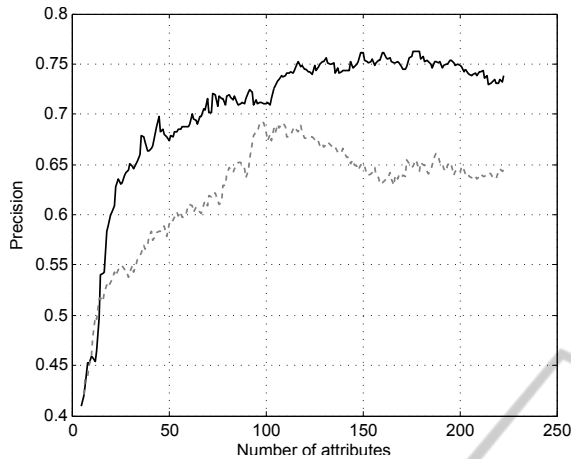


Figure 3: Attribute selection applied in Corel 1000 dataset. Black line: Attributed ranked according to a generic SVM classifier (WEKA(Hall et al., ) SMO implementation with standard parameters). Discontinuous line: Features transformed with PCA.

but SVM ranking provides considerably better results for a higher number of attributes. The best results of SVM ranking are 7% higher than those obtained by PCA. However, it is important to note that PCA is a much faster method than SVM ranking. This makes PCA appropriate for applications where time or computational performance is more critical than precision or where very short descriptors are needed (e.g. Very fast distance evaluations in massive datasets).

For a better understanding of the obtained feature space, the Bhattacharyya distance can provide a good overview related to the distances among different classes. Bhattacharyya distance for Gaussian multivariate distribution is given by (2). Assuming such distribution in the analyzed feature spaces, we can obtain an approximation about the distances among the different classes. The study of the relative distances provides significant information about their distribution and thus the discriminant potential when different classifiers are applied. As it can be observed in Table 2, the evaluated relative distance among classes fits with the errors shown in the confusion matrix.

$$D_B = \frac{1}{8} \Delta \mu' C^{-1} \Delta \mu + \frac{1}{2} \log \frac{\det(C)}{\sqrt{\det(C_1) \cdot \det(C_2)}} \quad (2)$$

where  $C = (C_1 + C_2)/2$

#### 4.1.2 Geoeye subset

Geoeye subset contains 1003 multi resolution satellite image patches categorized in 7 classes). All the Geoeye classes belong to geographical locations and include different cities as well as natural spaces. For this dataset, a precision of 94.51% has been obtained

Table 2: Bhattacharyya distance matrix for Corel 1000 dataset. Distance values corresponding to the two most similar classes according to the misclassification rates of the classification process are represented in bold.

	a	b	c	d	e	f	g	h	i	j
a	0	7.48	6.69	10.38	15.38	6.96	9.33	8.23	8.72	5.99
b	7.48	0	7.45	12.02	14.76	6.63	11.73	9.74	<b>6.27</b>	9.10
c	6.69	7.45	0	9.94	18.47	7.07	11.85	10.05	7.29	7.86
d	10.38	12.02	9.94	0	27.98	13.18	13.97	11.82	13.50	8.13
e	15.38	14.76	18.47	27.98	0	12.29	36.17	32.03	15.07	17.93
f	6.96	6.63	7.07	13.18	12.29	0	12.95	8.91	6.59	8.67
g	9.33	11.73	11.85	13.97	36.17	12.95	0	9.94	13.25	8.91
h	8.23	9.74	10.05	11.82	32.03	8.91	9.94	0	12.60	8.12
i	8.72	<b>6.27</b>	7.29	13.50	15.07	6.59	13.25	12.60	0	11.22
j	5.99	9.10	7.86	8.13	17.93	8.67	8.91	8.12	11.22	0

with the following parameter values:  $n_\phi = n_p 71$ , functional: *mean*. Comparing to the parameters employed in Corel 1000, the higher angular resolution has improved the rotational invariance of the descriptor adapting its behavior to the constraints of the dataset.

The final classification results have been tested using stratified 10-fold cross validation. Experimental text have demonstrated that Bayesian networks offer better precision rates than SVM for this specific dataset.

The results of the classification process are represented in Table 3 while Table 4 shows the Bhattacharyya distances among Geoeye dataset classes. As described in the previous case, there is a strong correspondence between the relative Bhattacharyya distance and the results obtained by using supervised classifiers (Bayesian networks in this case).

Table 3: Geoeye dataset confusion matrix. The closest classes attending the misclassification rates are represented in bold.

	a	b	c	d	e	f	g
(a) Athens	74	0	1	0	2	0	0
(b) Davis	0	183	0	0	2	7	2
(c) Manama	1	0	193	0	0	0	0
(d) Midway	2	0	0	62	1	0	0
(e) Nyragongo	0	0	4	0	77	2	2
(f) Risalpur	0	0	0	0	0	177	17
(g) Rome	0	0	1	0	0	<b>11</b>	182

#### 4.1.3 Subset of Caltech 101

A new test has been performed based on a subset of Caltech 101<sup>3</sup>. The classes contained in this subset and one sample per class are depicted in Figure 4. The dataset contains a different number of samples per

<sup>3</sup><http://www.vision.caltech.edu/archive.html>

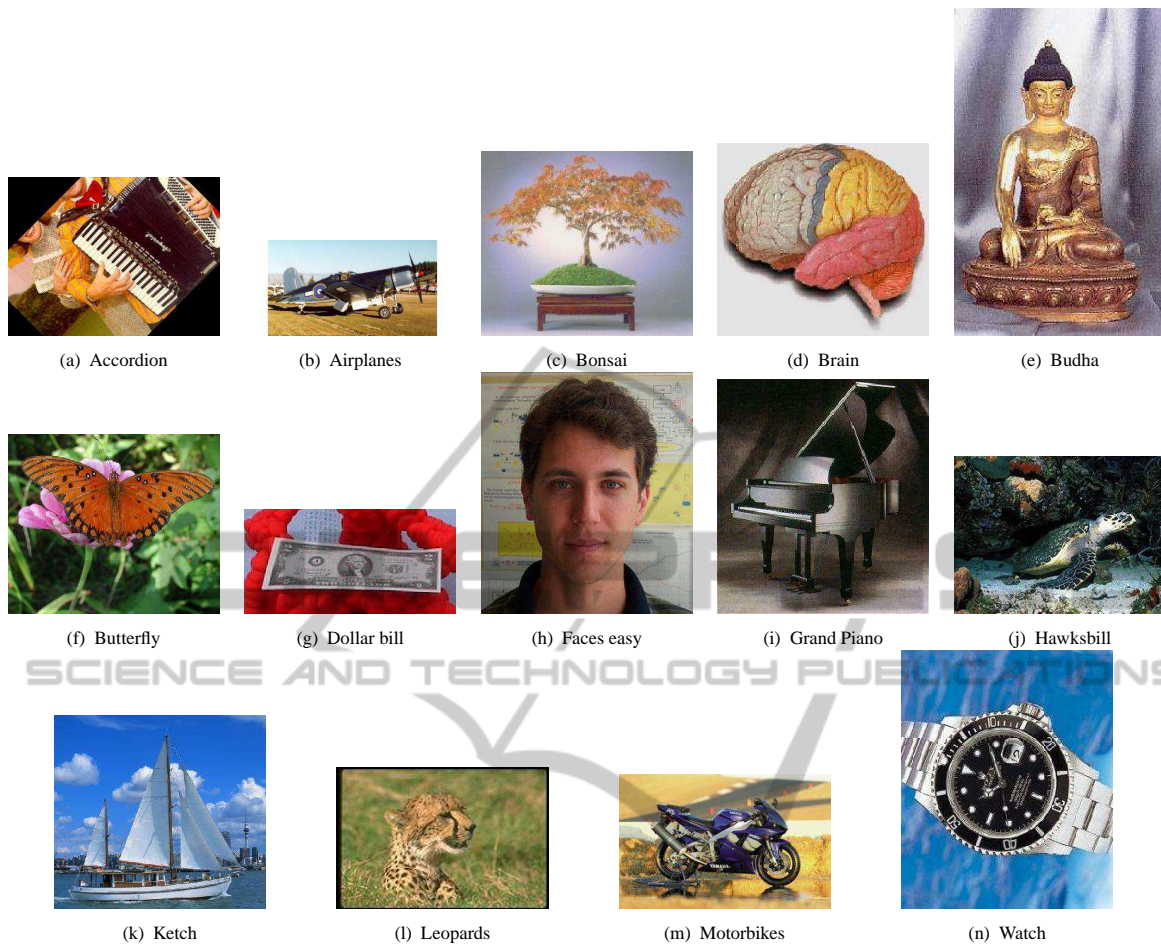


Figure 4: Samples of Caltech101 subset. The dataset includes an heterogeneous set of images at different resolutions and photogrametric conditions.

class and there is a high inter and intra class variation in many aspects such as resolution, image quality, color space, angle/perspective, scale etc. Figure 5 shows some samples of one of the Caltech 101 classes.

Table 4: Bhattacharyya distance matrix for Geoeeye dataset. Distance values corresponding to the two most similar classes according to the misclassification rates of the classification process are represented in bold.

	a	b	c	d	e	f	g
a	0	26.29	14.66	21.67	15.86	16.75	21.25
b	26.29	0	15.71	24.76	17.06	7.17	11.19
c	14.66	15.71	0	20.34	13.33	12.19	12.77
d	21.67	24.76	20.34	0	22.39	15.82	17.59
e	15.86	17.05	13.32	22.38	0	12.45	15.42
f	16.75	7.16	12.19	15.81	12.44	0	<b>5.15</b>
g	21.25	11.19	12.76	17.59	15.42	<b>5.15</b>	0

During this evaluation, we used DITEC method with the following parameters: functional=average value,  $n_{phi} = 100$ ,  $n_{rho} = 100$ ,  $n_{\xi} = 251$ . The num-

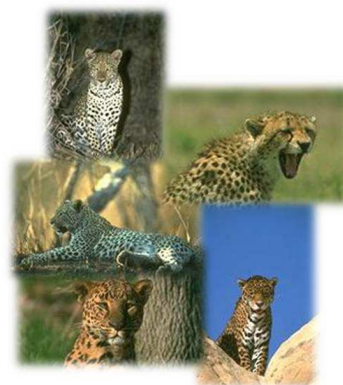


Figure 5: Some samples of images belonging to leopards class.

ber of DCT coefficients per channel was reduced to the first 80 positions, thus obtaining 480 descriptors per channel. Using the standard configuration of the Weka SMO classifier a precision of 79.8 % was obtained and reducing the number of dimensions to 75

Table 5: Caltech 101 subset confusion matrix.

	a	b	c	d	e	f	g	h	i	j	k	l	m	n
a	37	0	1	4	0	3	0	1	1	1	0	0	0	7
b	0	766	4	0	1	4	0	0	1	2	4	0	10	8
c	2	17	53	2	6	4	0	4	3	2	6	3	3	23
d	0	7	2	43	3	10	2	1	3	1	2	2	7	15
e	0	5	13	2	33	6	0	3	2	1	12	0	1	7
f	12	9	5	6	5	26	0	2	1	5	5	1	5	9
g	0	7	0	1	0	0	23	0	0	1	2	2	10	6
h	1	0	2	2	4	1	0	419	1	1	0	1	1	2
i	1	6	5	3	5	1	0	3	51	3	0	0	1	20
j	0	24	5	2	3	3	2	2	0	49	3	0	2	5
k	1	10	4	3	5	2	0	3	2	1	68	3	2	10
l	0	0	1	0	0	0	0	0	1	0	198	0	0	0
m	0	20	4	3	1	3	0	0	0	0	0	0	746	21
n	2	16	13	13	8	3	4	1	10	3	6	0	27	133

attributes by using a PCA decomposition, the precision was 76.4%. Both experiments were performed following a k-fold 10 cross-validation method. Table 5 shows the corresponding confusion matrix for SVM algorithm.

The Bhattacharyya distance of Caltech subset classes 6 cannot be directly calculated due to the singularity of the covariance matrix in some classes. Therefore, low variance attributes have been removed before the calculation. The obtained classification results are in general coherent to the Bhattacharyya distance specially for highest distances but the lower significance of this distance can be observed in some other cases. For example, the two classes with highest misclassification results (classes *m* and *n*) show a relatively high Bhattacharyya distance.

## 4.2 Behaviour as Local Descriptor

In addition to the evaluation of our DITEC approach running as global image descriptor, we also conducted an evaluation to measure how well this approach can be applied as a local image descriptor. We used our own framework based on the original work of (Mikolajczyk and Schmid, 2005) to evaluate our DITEC approach acting as a local descriptor. This framework is able to generate precision-recall curves as Mikolajczyk’s framework but is also able to generate more informative curves that represent the number or percentage of correct matches against specific values of a given transformation. We also used a set of images proposed by (Mikolajczyk and Schmid, 2005) and the image generator proposed in our framework. These

Table 6: Caltech 101 subset Bhattacharyya distance matrix (rounded values).

	a	b	c	d	e	f	g	h	i	j	k	l	m	n
a	0	31	27	16	17	16	35	28	29	18	29	29	16	26
b	31	0	10	24	23	24	29	14	12	19	10	7	18	7
c	27	10	0	21	22	22	35	8	10	20	10	10	19	7
d	16	24	21	0	10	10	29	23	25	11	23	25	9	20
e	17	23	22	10	0	11	27	23	25	10	24	23	9	20
f	16	24	22	10	11	0	29	24	26	11	22	24	9	21
g	35	29	35	29	27	29	0	36	35	24	35	33	23	30
h	28	14	8	23	23	24	36	0	11	22	11	12	22	8
i	29	12	10	25	25	26	35	11	0	22	14	13	20	8
j	18	19	20	11	10	11	24	22	22	0	21	20	8	17
k	29	10	10	23	24	22	35	11	14	21	0	8	21	9
l	29	7	10	25	23	24	33	12	13	20	8	0	22	9
m	16	18	19	9	9	9	23	22	20	8	21	22	0	17
n	26	7	7	20	20	21	30	8	8	17	9	9	17	0

sets of images show different geometric transformations such as in-plane rotation, scale similarity, and affine or projective transformations. All these sets of images allowed us to evaluate the robustness of our proposed descriptor against those types of transformations. Geometric transformations are related with the spatial transformations that occurs between different coordinate systems involved during image formation. Those transformation are mainly the Euclidean transformations, i.e. rotation and translation from world coordinate system to camera coordinate system, the projection of world points to camera coordinate system, and finally the points transformation to image coordinate system.

$$IF_2 = \left( \int |\xi(x)|^q dt \right)^r \quad (3)$$

As described in Section 3, DITEC is based on the generalization of the trace transform, and therefore a functional  $\Xi$  must be applied to every image to be transformed. In this case, we used  $IF_2$  functional (Equation 3) as defined in (Petrou and Kadyrov, 2004). All tests were carried out by comparing results obtained with DITEC approach with results obtained by the popular SURF (Bay et al., 2006b) descriptor in the same framework and datasets. The parameters of SURF descriptor were set as the default values implemented in OpenCV version (2.4).

We evaluated the DITEC performance as local image descriptor by measuring the matching ratio, i.e. percentage of correct matches of key points detected between the first image (reference image) and the rest of images in the dataset.

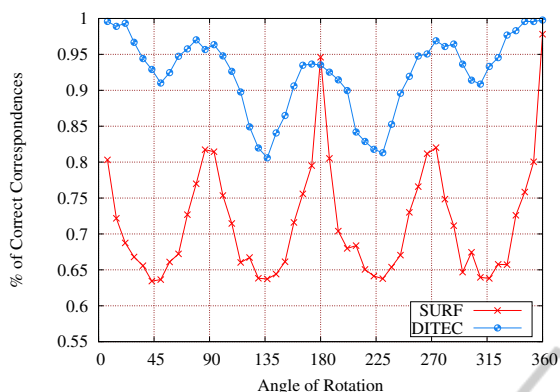


Figure 6: Results of in-plane rotation transformation test.

In order to evaluate the robustness of DITEC approach against rotation similarity transformation, we generated 50 in-plane rotated images, with 7.2 degrees of difference between consecutive images.

Figure 6 shows normalized correct matching ratio between source image with 0 degrees of rotation and the rest of images in the generated dataset. Both approaches show different responses given different angles. In the case of DITEC there are 4 local minimum points at  $\alpha = \frac{\pi}{4}, \frac{3\pi}{4}, \frac{5\pi}{2}$  and  $\frac{7\pi}{4}$  which are the points with highest distance to the reference values (considering that  $\alpha = \frac{\pi}{2}$  is closed to the reference). The chosen functional and the use of frequencial coefficients to represent the trace transform results provide a high rotational invariance. DITEC approach outperforms SURF by obtaining higher matching ratios along the transformation range, being always over an 80% of accuracy.

Next test shows the results of a similar evaluation process, but changing the rotation similarity transformation by a scale transformation. Similarly to the rotation transformation test, we generated 25 scale transformed images, with a scale range from 2 times the original size to a reduction of 2.5 times, as shown in Figure 7.

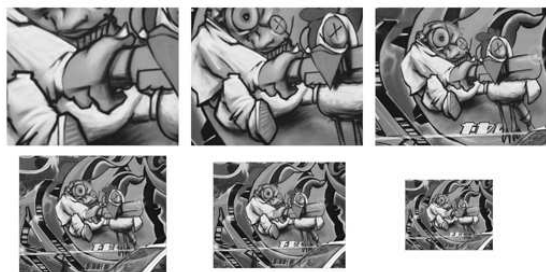


Figure 7: Scale transformed images of image 1 of Graffiti (Mikolajczyk and Schmid, 2005) dataset.

Figure 8 shows normalized results of scale transformation test. Both approaches show high robust-

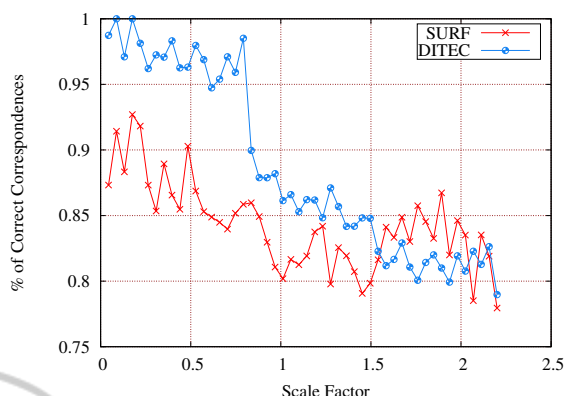


Figure 8: Normalized results of isotropic scale transformation test.

ness to scale transformation and DITEC obtains overall better results than SURF. Clearly, generalized trace transform with applied functional  $IF_2(3)$  shows great invariance capabilities against isotropic scale transformation.

In addition to previous test, where images were generated synthetically, the following tests use real images proposed in (Mikolajczyk and Schmid, 2005). These datasets are widely used by related community since its publication, and are composed of several sets of images performing different geometric and photometric transformations. Figure 9 shows images 1 to 4 of one of those dataset called *Boat*. Original dataset provides 2 more images, but in those images both SIFT and SURF detectors extract a very low number of points. Thus, normalized results are somehow distorted, therefore we decided to remove them from the evaluation. Images of Boat dataset show rotation, scale and projective transformations altogether.



Figure 9: Images 1-4 of boat dataset (Mikolajczyk and Schmid, 2005).

Results depicted in Figure 10 show how DITEC

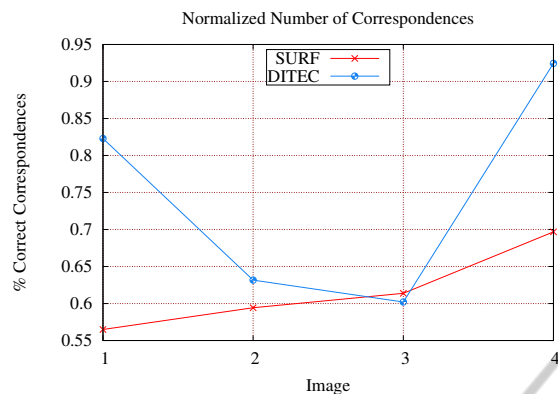


Figure 10: Results of images 1-4 of *Boat* dataset.

obtains high accurate ratios in every image, outperforming SURF approach.

As with *Boat* dataset, we used only first 3 out of 5 images due to the significant reduction of the number of extracted key points. This dataset shows mainly projective transformations between images, where all world points are on a same world plane. Results depicted in Figure 11 show that DITEC performs better than SURF approach, achieving higher accuracy ratios for every image. Even if DITEC is not projectively invariant, it is able to obtain good results in images where projective distortion is not very high with respect to reference image, such as in images 1 and 2, and thus can be locally approximated by an affinity. As described in (Petrou and Kadyrov, 2004), trace transform using specific functionals, such as  $IF_2$  (3) used in DITEC, can be robust against affine transformations.

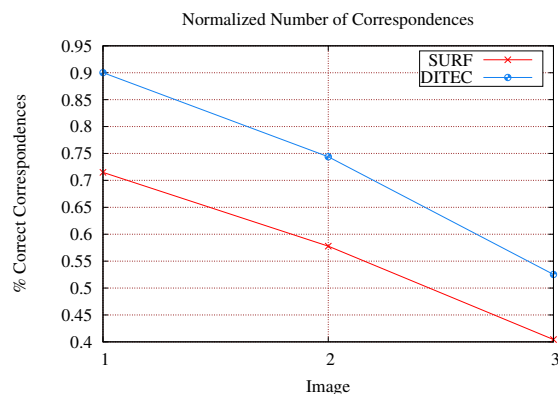


Figure 11: Results of images 1-3 of *Graffiti* dataset (Mikolajczyk and Schmid, 2005).

## 5 CONCLUSIONS

We have presented a new approach for both global and local image description. We have evaluated its

behavior with three domain characterization datasets considering DITEC as a global descriptor. The robustness of DITEC has been also evaluated performing local image description against several geometric transformations.

The discriminative power of the descriptor has been successfully evaluated with these three different datasets where complex objects and scenes have been correctly classified without any segmentation process or local description. Bhattacharyya distance has shown a good measure to characterize the feature space before any classification process which can be an efficient method for semi-supervised classification tasks. Moreover, the quality of the distance can be evaluated by analyzing the singularity of covariance matrices. These results make DITEC a very suitable method as a initial analysis algorithm for datasets where non *a priori* information exists.

DITEC performs well in in-plane rotation transformation and is almost invariant to scale transformation. In almost every test, DITEC approach outperforms SURF approach. It is worth mentioning that our current implementation of DITEC, acting as local image descriptor, is not optimized thus is currently slower than SURF descriptor. We think that current implementation can be severely improved by parallelizing the main loop of Radon transform because its computation is inherently parallel. Overall, results obtained with DITEC performing local description are very promising. We are currently conducting an in deep evaluation of DITEC local descriptor, by testing several parameters such as angular and radial resolution, number of frequencial coefficients and different functionals (instead of  $IF_2$ ), and comparing it with state-of-the-art descriptors such as BRISK, FREAK, or ORB among others.

## REFERENCES

- Ahmed, S., Khan, M., and Shahjahan, M. (2011). A filter based feature selection approach using lempel ziv complexity. In Liu, D., Zhang, H., Polycarpou, M., Alippi, C., and He, H., editors, *Advances in Neural Networks ISNN 2011*, volume 6676 of *Lecture Notes in Computer Science*, pages 260–269. Springer Berlin / Heidelberg. 10.1007/978-3-642-21090-7\_31.
- Bay, H., Tuytelaars, T., and Gool, L. V. (2006a). Surf: Speeded up robust features. In *In ECCV*, pages 404–417.
- Bay, H., Tuytelaars, T., and Van Gool, L. (2006b). Surf: Speeded up robust features. *Computer Vision–ECCV 2006*, pages 404–417.
- Bishop, C. M. (2006). *Pattern recognition and machine learning*. Springer, 1st ed. 2006. corr. 2nd printing edition.

- Bober, M. and Oami, R. (2007). Description of mpeg-7 visual core experiments. Technical report, ISO/IEC JTC1/SC29/WG11.
- Bouker, M. A. and Hervet, E. (2011). Retrieval of images using mean-shift and gaussian mixtures based on weighted color histograms. In *Proc. Seventh Int Signal-Image Technology and Internet-Based Systems (SITIS) Conf*, pages 218–222.
- Brasnett, P. and Bober, M. (2008). Fast and robust image identification. In *Proc. 19th Int. Conf. Pattern Recognition ICPR 2008*, pages 1–5.
- Calonder, M., Lepetit, V., Strecha, C., and Fua, P. (2010a). Brief: binary robust independent elementary features. In *Proceedings of the 11th European conference on Computer vision: Part IV, ECCV'10*, pages 778–792, Berlin, Heidelberg. Springer-Verlag.
- Calonder, M., Lepetit, V., Strecha, C., and Fua, P. (2010b). Brief: Binary robust independent elementary features. *Computer Vision—ECCV 2010*, pages 778–792.
- Cerra, D., Mallet, A., Gueguen, L., and Datcu, M. (2010). Algorithmic information theory-based analysis of earth observation images: An assessment. *IEEE J-GRSL*, 7(1):8–12.
- Fahmy, S. A. (2006). Investigating trace transform architectures for face authentication. In *Proc. Int. Conf. Field Programmable Logic and Applications FPL '06*, pages 1–2.
- Guyon, I., Weston, J., Barnhill, S., and Vapnik, V. (2002). Gene selection for cancer classification using support vector machines. *Mach. Learn.*, 46:389–422.
- Hall, M., Frank, E., Holmes, G., Pfahringer, B., Reutemann, P., and Witten, I. H. *SIGKDD Explor. Newsl.*, (1).
- Kadyrov, A. and Petrou, M. (1998). The trace transform as a tool to invariant feature construction. In *Proc. Fourteenth Int Pattern Recognition Conf*, volume 2, pages 1037–1039.
- Kadyrov, A. and Petrou, M. (2001). The trace transform and its applications. *IEEE J PAMI*, 23(8):811–828.
- Lin, S., Li, S., and Li, C. (2010). A fast electronic components orientation and identify method via radon transform. In *Proc. IEEE Int Systems Man and Cybernetics (SMC) Conf*, pages 3902–3908.
- Liu, N. and Wang, H. (2007). Recognition of human faces using discrete cosine transform filtered trace features. In *Proc. 6th Int Information, Communications & Signal Processing Conf*, pages 1–5.
- Liu, N. and Wang, H. (2009). Modeling images with multiple trace transforms for pattern analysis. *IEEE J SPL*, 16(5):394–397.
- Lowe, D. G. (1999). Object recognition from local Scale-Invariant features. *Computer Vision, IEEE International Conference on*, 2:1150–1157 vol.2.
- Manjunath, B. S., rainer Ohm, J., Vasudevan, V. V., and Yamada, A. (1998). Color and texture descriptors. *IEEE Transactions on Circuits and Systems for Video Technology*, 11:703–715.
- Martínez, J. M. (2004). Mpeg-7 overview, iso/iec jtc1/sc29/wg11 <http://mpeg.chiariglione.org/standards/mpeg-7/mpeg-7.htm>.
- Mikolajczyk, K. and Schmid, C. (2005). A performance evaluation of local descriptors. *Pattern Analysis and Machine Intelligence, IEEE Transactions on*, 27(10):1615–1630.
- Nasrudin, M. F., Petrou, M., and Kotoulas, L. (2010). Jawi character recognition using the trace transform. In *Proc. Seventh Int Computer Graphics, Imaging and Visualization (CGIV) Conf*, pages 151–156.
- O'Callaghan, R., Bober, M., and Oami, R. and Brasnett, P. (2008). Information technology - multimedia content description interface - part 3: Visual, amendment 3: Image signature tools.
- Olaizola, I. G., Quartulli, M., Flórez, J., and Sierra, B. (2012). Trace transform based method for color image domain identification. *arXiv*.
- Petrou, M. and Kadyrov, A. (2004). Affine invariant features from the trace transform. *IEEE J-PAMI*, 26(1):30–44.
- Peyrin, F. and Goutte, R. (1992). Image invariant via the radon transform. In *Proc. Int Image Processing and its Applications Conf*, pages 458–461.
- Seo, J. S., Haitsma, J., Kalker, T., and Yoo, C. D. (2004). A robust image fingerprinting system using the radon transform. *Sig. Proc.: Image Comm.*, 19(4):325–339.
- Shechtman, E. and Irani, M. (2007). Matching local self-similarities across images and videos. In *Proc. IEEE Conf. Computer Vision and Pattern Recognition CVPR '07*, pages 1–8.
- Snoek, C. G. M. and Smeulders, A. W. M. (2010). Visual-concept search solved? *Computer*, 43(6):76–78.
- Srisuk, S., Petrou, M., Kurutach, W., and Kadyrov, A. (2003). Face authentication using the trace transform. In *Proc. IEEE Computer Society Conf. Computer Vision and Pattern Recognition*, volume 1.
- Turan, J., Bojkovic, Z., Filo, P., and Ovsenik, L. (2005). Invariant image recognition experiment with trace transform. In *Proc. 7th Int Telecommunications in Modern Satellite, Cable and Broadcasting Services Conf*, volume 1, pages 189–192.
- Watanabe, T., Sugawara, K., and Sugihara, H. (2002). A new pattern representation scheme using data compression. *IEEE J-PAMI*, 24(5):579–590.